Proceedings of the Institute of Acoustics

A SYNTHETIC APERTURE SONAR MICRONAVIGATION KALMAN FILTER

JD Campbell Applied Signal Technology, Inc., Torrance, California, USA
JR Pearson Applied Signal Technology, Inc., Torrance, California, USA

1 INTRODUCTION

The redundant phase center (RPC) algorithm is used in multi-element SAS processing to remove cross track motion from recorded acoustic data. The RPC-estimated displacements, sometimes called micronavigation, also can be fused with other navigation data in an error state Kalman filter to obtain a theoretically optimal navigation solution. This technique was first introduced by Hansen et al[1] who evaluated various navigation data fusion techniques in terms of SAS image contrast.

In this paper, we present a unified approach for incorporating micronavigation measurements into a navigation Kalman filter. Our method addresses issues specific to RPC, including the timing of the transmit and receive events involved and the corrections originating from the navigator's resident KF. We begin by giving an overview of navigation Kalman filtering and aided inertial navigation. We then formulate an RPC model and derive the corresponding KF measurement model. Applicability to long-term navigation performance and to SAS motion compensation is discussed. Recommendations for future work are given.

2 KALMAN FILTERING FOR UNDERSEA NAVIGATION

The Kalman filter applies to partially observed linear Gaussian dynamic systems of the form

$$\begin{aligned} x_k &= \Phi_{k-1}x_{k-1} + u_{k-1} + w_{k-1} & w_k &\sim N(0, Q_k) \\ y_k &= H_k x_k + n_k & n_k &\sim N(0, R_k) \end{aligned} \tag{1}$$

The system state vector x_k is a hidden random process of interest that is observed indirectly through the measurement y_k. The variable Φ_k is the state transition matrix, u_k is control, and H_k is the measurement matrix. The system noise w_k and the measurement noise n_k are uncorrelated in time and $E[w_k n_j^T]=0$ for all j, k. For a model of the form (1), the Kalman filter provides a recursive estimator for the state x_k given measurements $y_1, y_2, \ldots, y_k$. The estimate $\hat{x}_k$ is optimal in both the maximum likelihood sense and the minimum mean square error sense. Additionally, the filter maintains the error covariance matrix $P_k = E[(x_k - \hat{x}_k)(x_k - \hat{x}_k)^T]$. The two types of operations carried out by the KF are extrapolation and update. Extrapolation (2) advances the state estimate and the error covariance over a time interval containing no measurements

$$\begin{aligned} \hat{x}_k &= \Phi_{k-1}\hat{x}_{k-1} + u_{k-1} & \hat{x}_0 &= E[x_0] \\ P_k &= \Phi_{k-1}P_{k-1}\Phi_{k-1}^T + Q_{k-1} & P_0 &= E\left[(x_0 - \hat{x}_0)(x_0 - \hat{x}_0)^T\right] \end{aligned} \tag{2}$$

The KF update (3) moves the state estimate and error covariance across a measurement by setting

$$\begin{aligned} \hat{x}_k &:= \hat{x}_k + K_k(y_k - H_k\hat{x}_k) \\ P_k &:= (I - K_k H_k)P_k \end{aligned} \tag{3}$$

where $K_k = P_k H_k^T \left(H_k P_k H_k^T + R_k\right)^{-1}$ is the Kalman gain. As can be seen by (1)-(3), the Kalman filter operates in discrete time.

Inertial navigators solve a nonlinear system of the form $\dot{\hat{\xi}}^{nav} = f^{nav}\left(\hat{\xi}^{nav}, \hat{s}^{imu}\right) + \sum_r \Delta\xi_r^{nav}\delta_r$, where $\hat{\xi}^{nav}$ is a state vector containing the navigation solution, f^{nav} describes the system dynamics, $\hat{s}^{imu}$ is imperfect sensor data from the inertial measurement unit (IMU), $\Delta\xi_r^{nav}$ are resets or corrections, and $\delta_r = \delta(t - t_r)$ is the Dirac delta function at correction time t_r. The corrections originate from a navigation Kalman filter and are applied periodically to the processor to improve the accuracy of $\hat{\xi}^{nav}$. The corresponding truth model is given by $\dot{\xi}^{nav} = f^{nav}\left(\xi^{nav}, s^{imu}\right)$, where ξ^{nav} is the true navigation state and s^{imu} is the output of a perfect IMU. By subtracting the truth model from the navigation model and exploiting the structure of f^{nav}, one may obtain a linear system of the form

$$\delta\dot{\xi}^{nav} = F^{nav}\delta\xi^{nav} + \sum_r \Delta\xi_r^{nav}\delta_r + w^{nav} \tag{4}$$

where $\delta\xi^{nav} = \hat{\xi}^{nav} - \xi^{nav}$ is the navigation error state vector, F^{nav} is the navigation error dynamics matrix, and w^{nav} is Gaussian white noise. The error dynamics matrix $F^{nav} = F^{nav}\left(\hat{\xi}^{nav}\right)$ is itself insensitive to error in $\hat{\xi}^{nav}$. The models contained in (4) include the standard navigation error equations and inertial sensor error models. The level of detail required in the modeling depends on the desired accuracy and the time duration involved. A detailed error model includes error states for position, velocity, and attitude and for sensor biases, scale factors, and misalignments. Gravity error models may also be included[2].

Suppose now that a navigation system is equipped with an aiding sensor whose output is related to the true navigation state ξ^{nav} and a true sensor state ξ^{aid} by

$$\hat{s}^{aid} = s^{aid} - n^{aid} \quad \text{where} \quad s^{aid} = h^{aid}\left(\xi^{nav}, \xi^{aid}\right) \tag{5}$$

Gaussian noise n^{aid} is uncorrelated between any two measurements and uncorrelated with system noise w. Now if h^{aid} is approximately linear about ξ^{nav} and ξ^{aid}, then we can form a quantity

$$y^{aid} = h^{aid}\left(\hat{\xi}^{nav}, \hat{\xi}^{aid}\right) - \hat{s}^{aid} \tag{6}$$

from available data $\hat{\xi}^{nav}$, $\hat{\xi}^{aid}$, and $\hat{s}^{aid}$ such that y^{aid} is related to the error states $\delta\xi^{nav}$ and $\delta\xi^{aid} = \hat{\xi}^{aid} - \xi^{aid}$ by

$$y^{aid} = H^{aid}\begin{pmatrix}\delta\xi^{nav} \\ \delta\xi^{aid}\end{pmatrix} + n^{aid} \tag{7}$$

where (7) follows from (5) and (6). The sensor errors in $\delta\xi^{aid}$ are typically modeled as Markov processes (including random walks and biases) so that we have $\delta\dot{\xi}^{aid} = F^{aid}\delta\xi^{aid} + w^{aid}$.

The combined error dynamics can now be described by the augmented system

$$\begin{pmatrix}\delta\dot{\xi}^{nav} \\ \delta\dot{\xi}^{aid}\end{pmatrix} = \begin{pmatrix}F^{nav} & 0 \\ 0 & F^{aid}\end{pmatrix}\begin{pmatrix}\delta\xi^{nav} \\ \delta\xi^{aid}\end{pmatrix} + \begin{pmatrix}\sum_r \Delta\xi_r^{nav}\delta_r \\ 0\end{pmatrix} + \begin{pmatrix}w^{nav} \\ w^{aid}\end{pmatrix} \tag{8}$$

The continuous time system (8) can be discretized using standard numerical techniques. The resulting discrete time system, together with measurement model (7) and measurements formed by (6), comprises a partially observed linear Gaussian system of the form (1) to which a Kalman filter can be applied. We note that the states of the resulting *navigation Kalman filter* consist only of

small, slowly-changing error quantities. The filter forms no direct estimates of whole value quantities such as latitude or longitude. Corrected whole value quantities are obtained by $\hat{\xi}^{nav} - \delta\hat{\xi}^{nav}$.

If the discretization times of system (8) are chosen to coincide with the correction times t_r of the control term $\sum_r \Delta\xi_r^{nav}\delta(t-t_r)$, then the discrete control term u_{k-1} in (1) and (2) becomes

$$u_{k-1} = \begin{cases} \Delta x_r & \text{if correction at time } t_k = t_r \\ 0 & \text{if no correction at time } t_k \end{cases} \qquad \text{where } \Delta x_r = \begin{pmatrix} \Delta\xi_r \\ 0 \end{pmatrix} \tag{9}$$

Thus, each correction is simply added on to the Kalman state at the appropriate time, and x_k in (1) and $\hat{x}_k$ in (2) represent post-correction quantities. In online KFs, a section of the correction vector is set to the negative of the corresponding section of the state vector. Thus, that section of the state vector is nulled each time a correction occurs. In KFs for data post processing, the Δx_r contain the correction history.

Extending the navigation KF from the single aiding sensor presented above to multiple aiding sensors is straightforward. For each additional sensor, the state vector in (7) and (8) is augmented with additional aiding states as needed, and the models are augmented accordingly. Each aiding sensor has a distinct measurement model of the form (7). As a new measurement becomes available from one of the aiding sensors, the KF is time propagated forward to the measurement's time of validity, and the KF is updated using the appropriate measurement model.

In the next section, it will be necessary to relate a measurement y to a linear combination of states that are valid at various times in the past. Consider a measurement model $y = H\begin{pmatrix} x^{current} \\ x^{stalled} \end{pmatrix} + n$, where the *stalled* states correspond to the current states at some previous time. If Φ is the transition matrix for x, then use of the augmented system

$$\begin{pmatrix} x_k^{current} \\ x_k^{stalled} \end{pmatrix} = \Phi_{k-1}^{aug}\begin{pmatrix} x_{k-1}^{current} \\ x_{k-1}^{stalled} \end{pmatrix} + \begin{pmatrix} w_{k-1} \\ 0 \end{pmatrix} + \begin{pmatrix} u_{k-1} \\ 0 \end{pmatrix} \tag{10}$$

provides a KF framework for y. Here, Φ_{k-1}^{aug} is $\begin{pmatrix} \Phi_{k-1} & 0 \\ 0 & I \end{pmatrix}$ or $\begin{pmatrix} \Phi_{k-1} & 0 \\ I & 0 \end{pmatrix}$, depending on whether the stalled states are to be maintained over the extrapolation step or whether they are to be replaced by more recent copies of the current states, respectively.

3 RPC AS A NAVIGATION AIDING SENSOR

For a given bistatic sonar, let p_T and p_R be the 3D transmit and receive position vectors, respectively, in some local coordinate system. Then, the phase center approximation (PCA) states that the bistatic sonar can be replaced by a fictitious monostatic sonar with phase center located at $p_{pc} = (p_T + p_R)/2$. The PCA is valid in the far field when $d_{bi}^2/(4rc) << 1$, where $d_{bi} = |p_R - p_T|$ is bistatic distance, r is range, and c is sound propagation speed. In the near field, the phase center approximation causes the received signal to be advanced by the small time interval $d_{bi}^2/(4rc)$. Taking this effect into account, the PCA holds in the near field when the transmission sector satisfies $d_{bi}^2(1-\cos^2\theta_e)/(4r\lambda_0) << 1$, where θ_e is the half transmission

beamwidth and λ_0 is wavelength at center frequency. Additionally, the bistatic angle d_{bi}/r should be small relative to the sensor beamwidths so that PCA does not affect directivity gains. These conditions are almost always valid for usual SAS systems[3].

In multi-element SAS, the sonar is operated so that each pair of consecutive pings contains one or more approximately redundant phase centers. The RPC algorithm estimates the time delay arising from the slant range displacement in a given phase center pair by finding the peak of the cross correlation of the two signals. Letting p_{pc}, p'_{pc}, d_{bi}, and d'_{bi} be the phase center positions and the bistatic distances of the first and second pings, respectively, and letting u_{slt} be the unit slant range vector directed from the scattering field toward the sonar, we obtain the following model for RPC time delay

$$\Delta\hat{t}^{rpc} = \Delta t^{rpc} - n^{rpc} \quad \text{where} \quad \Delta t^{rpc} = \frac{2}{c}\left(p'_{pc} - p_{pc}\right)\cdot u_{slt} + \frac{d'^2_{bi} - d^2_{bi}}{4rc} \tag{11}$$

Measurement noise n^{rpc} arises from noise in the recorded acoustic signals (and its arbitrary sign has been chosen to be negative). Since (11) comprises a sensor model of the form (5), we formulate the RPC KF measurement according to (6) as follows

$$y^{rpc} = \frac{2}{\hat{c}}\left(\hat{p}'_{pc} - \hat{p}_{pc}\right)\cdot \hat{u}_{slt} + \frac{\hat{d}'^2_{bi} - \hat{d}^2_{bi}}{4\hat{r}\hat{c}} - \Delta\hat{t}^{rpc} \tag{12}$$

where the hat symbol denotes quantities computed from available but imperfect data, i.e. corresponding to $\hat{\xi}^{nav}$, $\hat{\xi}^{aid}$, and $\hat{s}^{aid}$ in (6). Equation (12) can be interpreted as the difference between the INS-predicted time delay and the RPC-computed time delay.

It now remains to express (12) as a linear combination of error quantities that can be modeled in the KF. That is, we seek to obtain a relationship of form (7). Substituting (11) into (12) and neglecting second order terms, we obtain

$$\begin{aligned} y^{rpc} = &-\left[\frac{2}{\hat{c}}\left(\hat{p}'_{pc} - \hat{p}_{pc}\right)\cdot \hat{u}_{slt} + \frac{\hat{d}'^2_{bi} - \hat{d}^2_{bi}}{4\hat{r}\hat{c}}\right]s_c + \frac{2}{\hat{c}}\hat{u}_{slt}\cdot\left(\delta p'_{pc} - \delta p_{pc}\right) \\ &+ \frac{2}{\hat{c}}\left(\hat{p}'_{pc} - \hat{p}_{pc}\right)\cdot \delta u_{slt} + \frac{1}{2\hat{r}\hat{c}}\hat{p}'_{bi}\cdot\delta p'_{bi} - \frac{1}{2\hat{r}\hat{c}}\hat{p}_{bi}\cdot\delta p_{bi} + n^{rpc} \end{aligned} \tag{13}$$

where we have let $\Delta\hat{p}_{pc} = \hat{p}'_{pc} - \hat{p}_{pc}$ denote phase center displacement; s_c is the scale factor of sound propagation speed error defined by $\hat{c} = (1+s_c)c$; $\delta p_{pc} = \hat{p}_{pc} - p_{pc}$ and $\delta p'_{pc} = \hat{p}'_{pc} - p'_{pc}$ are phase center position errors on the first and second pings, respectively; $\delta u_{slt} = \hat{u}_{slt} - u_{slt}$ is error in the computed slant range direction; $p_{bi} = p_R - p_T$ and $\hat{p}_{bi} = \hat{p}_R - \hat{p}_T$ are the true and computed bistatic vectors, respectively, of the first ping; $\delta p_{bi} = \hat{p}_{bi} - p_{bi}$ is error in the computed bistatic vector of the first ping; and similarly $\hat{p}'_{bi}$ and $\delta p'_{bi}$ are the computed bistatic vector and the bistatic vector error, respectively, of the second ping. We note that (13) is a linear combination of error quantities, which is a significant step toward achieving (7). Each error quantity of (13) is now analyzed in turn.

A model for sound speed error s_c depends on the method of computing $\hat{c}$. If $\hat{c}$ is assumed to be 1500m/s, then the model for s_c should include a random bias component. Additionally, the model may include a first order Markov process whose strength and correlation time are functions of the

spatial statistics of sound speed variation coupled through vehicle velocity. Thus, a reasonable model for s_c augments the system state vector by one or two states.

Writing out phase center position error term, we find $\delta p'_{pc} - \delta p_{pc} = \left(\delta p'_T + \delta p'_R - \delta p_T - \delta p_R\right)/2$, which is a sum and difference of errors in the computed sensor positions. A given sensor position may be decomposed into an INS position and a lever arm from the INS to the sensor by $p_{sen} = p_{ins} + p_{lev}$. For convenience, we now introduce the index $j = 1,2,3,4$ to indicate the following four events: 1) first ping transmit, 2) first ping receive, 3) second ping transmit, and 4) second ping receive. Thus, the second dot product in (13) becomes

$$\hat{u}_{slt} \cdot \left(\delta p'_{pc} - \delta p_{pc}\right) = \tfrac{1}{2}\sum_j (-1)^{\lceil j/2 \rceil} \hat{u}_{slt}^T \delta p_{ins}(t_j) + \tfrac{1}{2}\sum_j (-1)^{\lceil j/2 \rceil} \hat{u}_{slt}^T \delta p_{lev}(j) \qquad (14)$$

where $\lceil \cdot \rceil$ is the ceiling operator, i.e. $\sum_j (-1)^{\lceil j/2 \rceil} a_j = -a_1 - a_2 + a_3 + a_4$ for a given sequence a_j. Position error at the INS, δp_{ins}, is already a block of three states contained in the system state vector, within the navigation block $\delta\xi^{nav}$. Since δp_{ins} enters into the measurement equation at four different times, the system state vector must be augmented with position error stalled states at each relevant time using the technique described by (10). We note that the first sum in (14) loosely represents the growth in the navigation system slant range position *error* over one ping interval. It is the key term in the RPC measurement model. The second sum in (14) can be expanded as follows. Letting superscripts *n* and *b* denote coordinatization in the NED and body frames, respectively, we have $p_{lev}^n(j) = C_b^n(t_j) p_{lev}^b(j)$ where C_b^n is the body-to-NED direction cosine matrix. We note that the body frame transmit lever arm is stationary, i.e. $p_{lev}^b(1) = p_{lev}^b(3)$, and the body frame receive lever arms $p_{lev}^b(2)$ and $p_{lev}^b(4)$ are separated by roughly twice the advance distance between the two pings. The exact value of $p_{lev}^b(4)$ may lie in-between receivers if along track interpolation is used in computing the second signal in the RPC cross correlation. Taking the variation of $p_{lev}^n(j)$, we can show that

$$\hat{u}_{slt}^T \delta p_{lev}(j) = \left[\hat{u}_{slt}^n \times \left(\hat{C}_b^n \hat{p}_{lev}^b(j)\right)\right]^T \psi^n + \left(\hat{u}_{slt}^n\right)^T \hat{C}_b^n \delta p_{lev}^b(j)$$

where ψ^n is navigation system attitude error and where the time-dependency in $\hat{C}_b^n$ and ψ^n has been suppressed since these quantities change very little over a single ping interval. We note that ψ^n is already modeled within the navigation block $\delta\xi^{nav}$ of the system state vector. The second sum in (14) is then given by

$$\tfrac{1}{2}\sum_j (-1)^{\lceil j/2 \rceil} \hat{u}_{slt}^T \delta p_{lev}(j) = \tfrac{1}{2}\left[\hat{u}_{slt}^b \times \left(\hat{p}_{lev}^b(4) - \hat{p}_{lev}^b(2)\right)\right]^T \hat{C}_n^b \psi^n + \tfrac{1}{2}\left(\hat{u}_{slt}^b\right)^T \left(\delta p_{lev}^b(4) - \delta p_{lev}^b(2)\right) \qquad (15)$$

If we assume that the receive array is nominally aligned with the vehicle forward axis, then the term $\hat{p}_{lev}^b(4) - \hat{p}_{lev}^b(2)$ can be written as $-2\hat{d}_{adv}\hat{u}_{fwd}^b$ where $\hat{d}_{adv}$ is distance of advance between pings and $\hat{u}_{fwd}^b = \begin{pmatrix}1 & 0 & 0\end{pmatrix}^T$ is the unit forward vector. Similarly, the last term on the right hand side of (15) can be simplified to $-\hat{d}_{adv}\left(\hat{u}_{2D-orth}^b\right)^T \alpha$, where $\hat{u}_{2D-orth}^b$ is the last two components of the unit slant-plane orthogonal vector $\hat{u}_{orth}^b = \hat{u}_{slt}^b \times \hat{u}_{fwd}^b$ and $\alpha = \begin{pmatrix}\alpha_p & \alpha_y\end{pmatrix}^T$ is the last two components (pitch and yaw) of the misalignment in the array-to-body transformation used to compute the $p_{lev}^b(j)$. We therefore augment the system state vector with the array misalignment α and model it as a random constant. Compiling results, (14) becomes

Formatted: Justified

Formatted: Justified

$$\hat{u}_{slt}\cdot\left(\delta p'_{pc}-\delta p_{pc}\right)=\tfrac{1}{2}\sum_j(-1)^{\lceil j/2\rceil}\hat{u}_{slt}^T\delta p_{ins}(t_j)-\hat{d}_{adv}\left(\hat{u}_{orth}^n\right)^T\psi^n-\hat{d}_{adv}\left(\hat{u}_{2D-orth}^b\right)^T\alpha \qquad (16)$$

The second and third terms of (16) represent an artificial slant range crabbing effect arising from sensor misalignments.

The slant range direction error δu_{slt} arises from multiple sources and couples with the phase center displacement $\Delta\hat{p}_{pc}$ in (13). The slant range vector itself may be written as $u_{slt}^n=C_b^nC_s^bu_{slt}^s$, where the sonar frame *s* is aligned with the body frame *b* to within a small angle rotation and the slant range vector is given by $u_{slt}^s=\begin{pmatrix}0 & (-1)^{dir}\cos\theta_{slt} & \sin\theta_{slt}\end{pmatrix}^T$ where *dir* is 0 for port-facing sonar data and 1 for starboard-facing data and θ_{slt} is the slant range depression angle of the RPC measurement's range subswath. Then, taking the variation of u_{slt}^n we find

$$\Delta\hat{p}_{pc}^n\cdot\delta u_{slt}^n=\left(\Delta\hat{p}_{pc}^n\times\hat{u}_{slt}^n\right)^T\psi^n+\left(\Delta\hat{p}_{pc}^b\times\hat{u}_{slt}^b\right)^T\mu+\left(\Delta\hat{p}_{pc}^n\right)^T\hat{u}_{orth}^n\delta\theta_{slt} \qquad (17)$$

where μ is misalignment in the computed sonar-to-body transformation and $\delta\theta_{slt}$ is the (scalar) slant range angle error. The quantity μ arises from misalignment of the sonar maximum response axis. The term $\left(\Delta\hat{p}_{pc}^b\times\hat{u}_{slt}^b\right)^T\mu$ is negligible for usual SAS systems since the first component of each vector in the triple product will be nearly zero, as we now show. Vehicle speed and PRI are typically controlled so as to null the forward part of $\Delta\hat{p}_{pc}^b$. The body frame slant range $\hat{u}_{slt}^b$ is nominally aligned with u_{slt}^s which has no forward component. Lastly, the first component of μ is negligible as long as sonar directivity is relatively invariant over the depression angle extent of the range subswath. The slant angle error $\delta\theta_{slt}$ in (17) arises from imperfect knowledge of bathymetry and, to a lesser extent, displacement of the subswath acoustic center due to range-dependent variation in bottom reflectivity. The error $\delta\theta_{slt}$ couples through the component of vehicle motion $\Delta\hat{p}_{pc}$ that is orthogonal to the slant plane. In order to minimize $\delta\theta_{slt}$, the angle $\hat{\theta}_{slt}$ should be computed from bathymetry maps or onboard interferometric processing. Since developing a dynamic model for $\delta\theta_{slt}$ is beyond the scope of this paper, we assume $\left(\hat{u}_{orth}^n\right)^T\Delta\hat{p}_{pc}^n\delta\theta_{slt}$ is white noise and combine it with the RPC algorithm noise n^{rpc}.

The bistatic vector error terms $\hat{p}_{bi}\cdot\delta p_{bi}/(2\hat{r}\hat{c})$ and $\hat{p}'_{bi}\cdot\delta p'_{bi}/(2\hat{r}\hat{c})$ in (13) are negligible in usual SAS systems. They represent growth of along-track position error between transmit and receive, scaled by the bistatic angle, and their difference is approximately $\hat{d}_{adv}\delta v_{fwd}/\hat{c}^2$. Converting to range, this quantity is of the order 10 microns for systems with good along-track velocity accuracy.

Collecting results together, we obtain the following RPC measurement model

$$\begin{aligned}y^{rpc}=(\hat{c}/2)\Big\{&\tfrac{1}{2}\sum_{j=1}^4(-1)^{\lceil j/2\rceil}\hat{u}_{slt}^T\delta p_{ins}(t_j)+\left(-\hat{d}_{adv}\hat{u}_{orth}^n+\Delta\hat{p}_{pc}^n\times\hat{u}_{slt}^n\right)^T\psi^n\\&-\hat{d}_{adv}\left(\hat{u}_{2D-orth}^b\right)^T\alpha-\left[\Delta\hat{p}_{pc}\cdot\hat{u}_{slt}+\left(\hat{d}_{bi}'^2-\hat{d}_{bi}^2/8\hat{r}\right)\right]s_c\Big\}+\nu^{rpc}\end{aligned} \qquad (18)$$

having the desired form of (7), where $\nu^{rpc}=\left(\hat{u}_{orth}^n\right)^T\Delta\hat{p}_{pc}^n\delta\theta_{slt}+n^{rpc}$ is the effective measurement noise. Variance of the cross-correlation noise n^{rpc} can be computed from the cross-correlation coefficient using the Cramer-Rao lower bound or the more general Ziv-Zakai lower bound[4,5].

4 DISCUSSION

The approach described in the previous section incorporates RPC-computed delays into an error state navigation Kalman filter. The RPC-specific states include stalled position errors for transmit and receive events over the past two pings, array misalignment, and sound speed error. As each RPC delay becomes available, an RPC divergence is computed by (12) and the KF is updated using (18). If, in addition to RPC measurements, the KF also includes measurements from the other available navigation sensors such as DVL, depth gauge, and GPS, then this approach represents an optimal data fusion technique for combining SAS-derived micronavigation and conventional navigation sensors.

Two possible architectures for implementing the KF are shown in Fig 1. The real-time implementation depicted on the left follows the conventional Kalman aiding scheme. Here, data from the Navigation Aids, including RPC Displacements, are differenced with data from the Navigator in order to compute the Divergences. The Divergences are input to the KF as observations. Periodic corrections are applied from the KF to the Navigator, which provides the Navigation Solution. The post-processing architecture is shown on the right. Here, it is assumed that the AUV is equipped with an Organic Navigator and KF. The purpose of the Micronav KF is to estimate the error in the Organic Navigation Solution using data computed from the Navigation Aids and RPC. (In addition to estimating navigation error, the Micronav KF also estimates aiding the sensor parameters such as biases, scale factors, misalignments, etc.) The estimates are shown as output Corrections from the Micronav KF. In order to properly implement the error state system (8), the Micronavigation KF requires input Corrections from the Organic KF. These Organic KF Corrections provide the $\Delta\xi_r^{nav}$ in (8). Since (8) provides an exact description of the system error dynamics for both architectures, the post-processing architecture is fundamentally equivalent to the real-time architecture in terms of validity and accuracy.

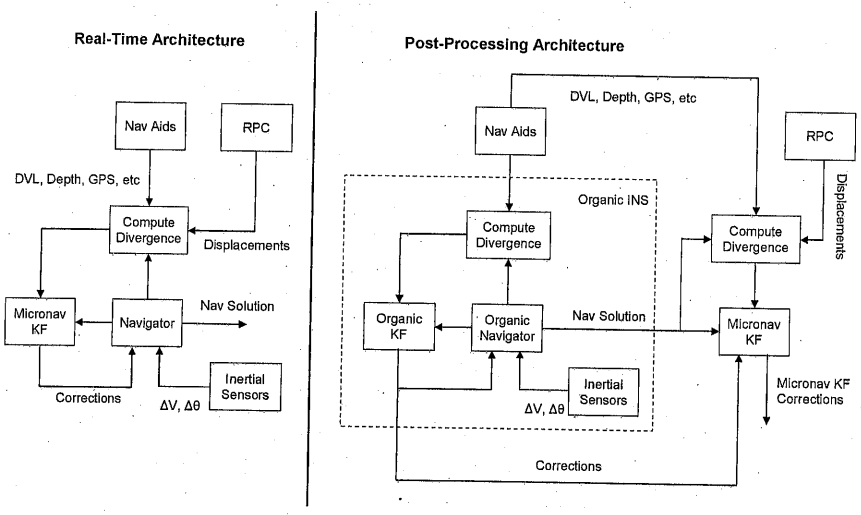

Figure 1. Real-Time and Post-Processing Architectures

The micronavigation KF with RPC aiding was originally conceived as a means for improving long-term navigation performance. Simulation thus far has shown that the effectiveness of RPC aiding

depends on the characteristics of the underlying navigation system. For the high accuracy navigation systems used in undersea surveys, it does not appear that micronavigation aiding is able to improve the system's ability to gyrocompass and maintain heading accuracy. Heading error resulting from gyro bias is a primary source of position error for long-term vehicle operation without an absolute position reference. On the other hand, RPC behaves similarly to the cross track components of the DVL. Thus, micronavigation aiding provides some redundancy in the case of DVL failure and could be used in calibrating a new DVL in case of at-sea replacement. In systems where DVL error dominates gyro-induced errors, RPC measurements can provide some performance enhancement.

An alternative application of the micronavigation KF is SAS motion compensation. As no single source of mocomp data is ideal under all conditions, the KF provides an attractive framework for blending data from all available sources. Several lines of research related to mocomp are elaborated in the next section.

5 RECOMMENDATIONS

First, although only the slant range component of phase center displacement was considered in this analysis, it is also possible to estimate the along track, or surge, displacement by maximizing signal correlation in the along-array direction. The surge estimator is far less accurate than the slant range sway estimator; however, surge estimates have the interesting property of being independent of sound speed. Thus, RPC-derived surge may provide the KF with observability into the forward component of accelerometer and DVL scale factors. Second, if the micronavigation KF solution shows promise for SAS mocomp, then further improvement may be achieved by replacing the KF with a fixed interval Kalman smoother over each SAS data frame. The smoothed solution has lower variance than the filtered solution and is not subject to discontinuities at the KF updates. Third, there is the possibility of using autofocus as an aiding sensor. Autofocus-estimated phase errors provide a measure of residual slant range motion in the navigation solution used to focus the image. They may contain valuable information about inertial instrument errors. Fourth, a micronavigation KF may provide the means for detecting and correcting $\lambda_0/2$ cycle slips which occur in the RPC algorithm at low SNR. A general property of KFs is that the innovation sequence $y_k - H_k\hat{x}_k$ in (3) is white noise with covariance matrix $R_k + H_k P_k H_k^T$. In the case of the RPC measurement, the covariance matrix of the innovation is a scalar quantity and the corresponding standard deviation is typically a small fraction of a wavelength. Thus, it should be possible to detect and remove cycle skip errors by thresholding on the KF innovation.

We would like to thank Mark D. Tinkle of Applied Signal Technology, Inc. for proposing and investigating the use of stalled states in the Kalman filter. This work was funded by the Office of Naval Research, contract number N00014-05-C-0028.

6 REFERENCES

1. R.E. Hansen, T.O. Sæbø, K. Gade, and S. Chapman, Signal processing for AUV based interferometric synthetic aperture sonar, Proc. MTS/IEEE OCEANS 2003 (5), 2438-2444, San Diego, CA (Sep 2003).
2. C. Jekeli, Inertial navigation systems with geodetic applications, Walter de Gruyter, New York (2000).
3. A. Bellettini and M.A. Pinto, Theoretical accuracy of synthetic aperture sonar micronavigation using a displaced phase-center antenna, IEEE J. of Oceanic Eng. (27)4, 780-789 (Oct 2002).
4. Weiss, A.J. and E. Weinstein, Fundamental limitations in passive time delay estimation—Part 1: Narrow-band systems, IEEE Trans. ASSP (31)2, 472-486 (Apr 1983).
5. J.D. Campbell and E. Chang, Concepts for synthetic aperture sonar performance prediction and mission planning, MTS/IEEE OCEANS, Washington, DC (Sep 2005).